Optimization in the Multi-element Synthetic Transmit Aperture Method for Ultrasound Imaging

Yuriy Tasinkevych, Ihor Trots, and Andrzej Nowicki

Abstract The paper deals with optimization of the transmit aperture in the multi-element synthetic transmit aperture method (MSTA) for ultrasound imaging. In contrast to the conventional synthetic transmit aperture (STA) method, MSTA allows to increase the system frame rate and provides the best compromise between penetration depth and lateral resolution.

The optimal choice of the transmit sub-aperture size and the aperture shift between subsequent transmissions is the most important question for efficient imaging with MSTA algorithm. Here the results of the analysis obtained by the developed optimization algorithm are presented. Maximum penetration depth and best lateral resolution at given depths were chosen as the optimization criteria. The numerical experiments were carried out in the MATLAB® environment for 128-element linear transducer array with 0.48 mm inter-element spacing excited by one sine cycle burst of the nominal frequency of 5 MHz. The wire phantom was simulated by FIELD II program. The transmit apertures up to 16 element wide were considered.

Keywords Synthetic aperture • Ultrasound imaging • Beam-forming

Y. Tasinkevych (✉)
Department of Physical Acoustics, Institute of Fundamental Technological Research of the Polish Academy of Sciences, 5B Pawińskiego str., Warsaw 02-106, Poland
e-mail: yurijtas@ippt.gov.pl

I. Trots • A. Nowicki
Department of Ultrasound, Institute of Fundamental Technological Research of the Polish Academy of Sciences, 5B Pawińskiego str., Warsaw 02-106, Poland

A. Nowicki et al. (eds.), *Acoustical Imaging*, Acoustical Imaging 31,
DOI 10.1007/978-94-007-2619-2_15,

1 Introduction

Ultrasound imaging has become one of the primary techniques for medical imaging mainly due to its accessibility, non-ionizing radiation, and real-time visualization. The highest possible image quality which is required to make it suitable for clinical diagnostics can be achieved by using array transducers and advanced beam-forming techniques. However this usually requires using several transmit beams focused at different depth at the cost of frame rate decrease. Synthetic aperture (SA) imaging may offer a solution to this problem. The SA method has become one of the most perspective and promising techniques in nowadays medical ultrasound imaging systems. Synthetic aperture is a post-processing reconstruction technique which uses a single or multiple elements transducer radiation pattern to synthesize the effect of larger aperture. Several methods were proposed to form a synthetic aperture in ultrasound imaging. Among them the synthetic transmit aperture (STA) technique [1–3], which uses a single element transmit aperture, is the one providing the full dynamic focusing in both transmit and receive modes, thus giving the highest imaging quality. In contrast to STA algorithm, the multi-element synthetic transmit aperture (MSTA) [4, 5], using a small number of elements in transmit mode, allows to increase the system frame rate and provides the best compromise between penetration depth and lateral resolution as compared to the STA method. The main problem which arise in the MSTA method is an optimal choice of the transmit sub-aperture size and the shift between subsequent transmissions.

The paper presents the results of the analysis obtained by the developed optimization algorithm. The number of elements used in transmit mode and the aperture shift were optimized using the criteria of maximum penetration depth and maximum lateral resolution at given depths. The optimization was carried out in the MATLAB® environment using the FIELD II [6, 7] program for wire phantom data simulation. The 128-element linear transducer array with 0.48 mm inter-element spacing excited by one sine cycle burst of the nominal frequency of 5 MHz and the sampling rate of 50 MHz was assumed in the numerical experiments. The preliminary results show that the optimal aperture size depends on the required visualization depth and acceptable decrease in the lateral resolution.

2 Multi-element Synthetic Transmit Aperture Method

The multi-element synthetic transmit aperture method originates from the conventional synthetic transmit aperture which is sketched out in Fig. 1a. The STA can be used as an alternate to the conventional phased array imaging technique. It provides for the full dynamic focusing both in transmit and receive modes yielding the highest imaging quality.

In this method a full large aperture is synthesized by multiple transmissions. At each time a single element is used to emit unfocused wave-field. The backscattered

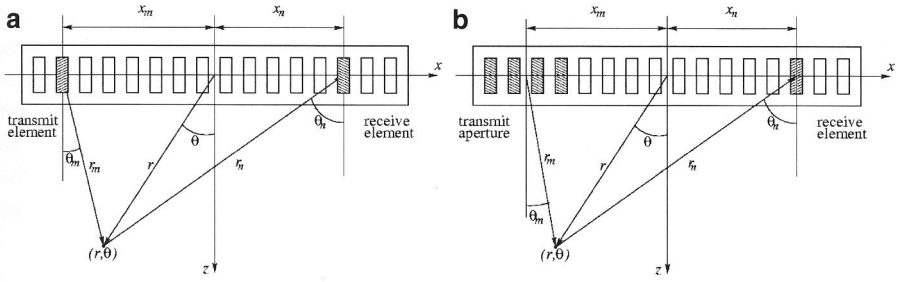

Fig. 1 Transmit and receive elements combination and the focal point in (**a**) STA method, (**b**) MSTA method

waves are received by each element independently and the resulting RF echoes are digitized and stored in memory. For an N-element array, $N \times N$ independent recordings are required to synthesize an N-element phased array in both transmit and receive modes. After finishing the full data acquisition cycle the RF echoes are summed up with properly chosen time delays according to the focal point spatial position (see Fig. 1a). Thus, in the case of N-element array for each point in the image, the A-scan signal can be expressed as follows:

$$A_{STA}(r,\theta) = \sum_{m=1}^{N}\sum_{n=1}^{N} y_{m,n}\left(\frac{2r}{c} - \tau_{m,n}\right), \tag{1}$$

where $y_{m,n}(t)$ is the RF echo signal and $\tau_{m,n}$ is the round-trip delay, defined for the (m, n) transmit-receive element combination by the following expression:

$$\tau_{m,n} = \tau_m + \tau_n, \quad 1 \le m, n \le N. \tag{2}$$

The corresponding delays for m'th and n'th element relative to the imaging point (r, θ) are:

$$\tau_i = \frac{1}{c}\left(r - \sqrt{r^2 + x_i^2 - 2x_i r\sin\theta}\right), \quad i = m, n, \tag{3}$$

where x_m, x_n are the positions of the m'th and n'th elements, respectively, and r, θ are the polar coordinates of the imaging point with respect to the origin placed in the center of the transducer's aperture. In contrast to the STA method, in the MSTA approach at each emission a multiple-element transmit aperture is used as illustrated in Fig. 1b. In the receive mode both methods are equivalent. The main advantage of the MSTA algorithm is the improvement of lateral resolution and visualization depth of the resulting image. For the N-element array and N_t-element transmit aperture there are $M = N/N_t$ emissions in a cycle altogether, if it is assumed that the transmit aperture is shifted by $N_{sh} = N_t$ elements between

subsequent emissions. It should be noted, that if $N_{sh} < N_t$ is applied, the higher image quality can be obtained. However the number of emissions M increases, which leads to the frame rate decrease as compared to the case $N_{sh} = N_t$. Consequently, for N-element aperture, $M \times N$ data recordings are required for image reconstruction. As in the case of the STA, the final high resolution image is synthesized by summing up of all received RF echoes upon completion of the data acquisition cycle. In the case of N-element array for each point in the image the A-scan signal can be expressed by a similar expression as in Eq. 1:

$$A_{MSTA}(r,\theta) = \sum_{m=1}^{M}\sum_{n=1}^{N} y_{m,n}\left(\frac{2r}{c} - \tau_{m,n}\right). \tag{4}$$

The round-trip delay $\tau_{m,n}$ in the case of MSTA method is defined for the (m, n) transmit-receive pair by Eqs. 2 and 3. The transmit element delay is evaluated from Eq. 3, where x_m now stands for the transmit aperture center position. The frame rate is increased in the MSTA by N_t as compared to the STA method due to decrease of the total number of emissions which speeds up the data acquisition process. Unfortunately, it appears that too excessive increasing of the transmit aperture size N_t (and its shift at the same time) leads to worsening of the lateral resolution. However, using a small number of elements in transmit mode allows to increase the system frame rate and provides the best compromise between penetration depth and lateral resolution as compared to the STA method. The optimal choice of the transmit sub-aperture size is crucial in the MSTA method. In the next section the corresponding optimization problem is considered for the MSTA algorithm.

3 Optimization Problem for MSTA Method

In this section the algorithm for optimal choice of the transmit aperture size in MSTA method is discussed. For the conventional MSTA which is mainly considered here the transmit aperture shift between subsequent transmissions equals its size: $N_{sh} = N_t$. The developed algorithm, however, can be extended to the more general case of the MSTA method with different values of the shift N_{sh}. Usually, $N_{sh} < N_t$ yields some improvement of the synthesized image quality at the cost of the frame rate decrease.

In the considered algorithm the maximum penetration depth and best lateral resolution at given depths are chosen as optimization criteria. The 2D ultrasound image of thin wire phantom is simulated in FIELD II program for Matlab® for each size of the transmit aperture. The reflectors in the phantom are located in the nodes of a rectangular grid. The rows and columns are equidistantly spaced. For each individual experiment the lateral resolution and penetration depth are estimated. The lateral resolution is evaluated for each lateral cross section coinciding with the rows of the phantom. In the case of the algorithm presented

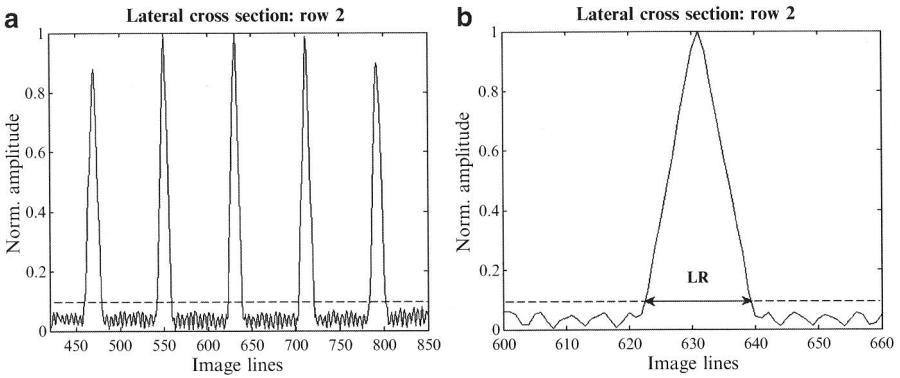

Fig. 2 Evaluation of the lateral resolution for given row: LR is a number of image lines for which the normalized amplitude is above a chosen threshold level for the reflector located at the intersection of the row and central column in the phantom

here only the reflector located at the central column is taken into account for simplicity. This column corresponds to the transducer aperture center position. For convenience the lateral cross sections are labelled here in accordance with the phantom row numbers (10 rows in the example considered in the next section). The lateral resolution in the presented algorithm is estimated as a number of image lines for which the normalized (with respect to the maximum value in a given lateral cross section) amplitude exceeds the minimal chosen threshold level (0.1 in the examples considered in the next section) for the reflector located at an intersection of a given row and the central column of the phantom (see Fig. 2 for explanation).

The penetration depth is estimated in a similar manner. For the central column of the phantom the penetration depth is assessed by the relative amplitude of the reflected signal of the deepest visible reflector for which the corresponding normalized (with respect to the maximum value in the considered axial cross section) amplitude exceeds the minimum threshold level (0.2 in the examples considered in the next section), as illustrated in Fig. 3. Below this level the reflectors are assumed to be indistinguishable. In the examples shown in Figs. 2 and 3 which explain the optimization algorithm performance, the STA algorithm was exploited for visualization, that is, a single-element aperture was used in transmit and receive modes. For smooth visualization of the lateral cross sections the interval between subsequent image lines was chosen 0.1 of the transducer pitch (10 image lines per transducer pitch), similarly as in the examples presented in the next section. After estimation of the lateral resolution and penetration depth the optimal system configuration is selected. Two different approaches are realized in the presented algorithm. The first seeks for that transmit aperture configuration yielding the maximum penetration depth for lateral resolution being within some tolerance bounds. The second approach, on the other hand, selects the configuration giving the best lateral resolution for penetration depth not less then some minimum acceptable limit.

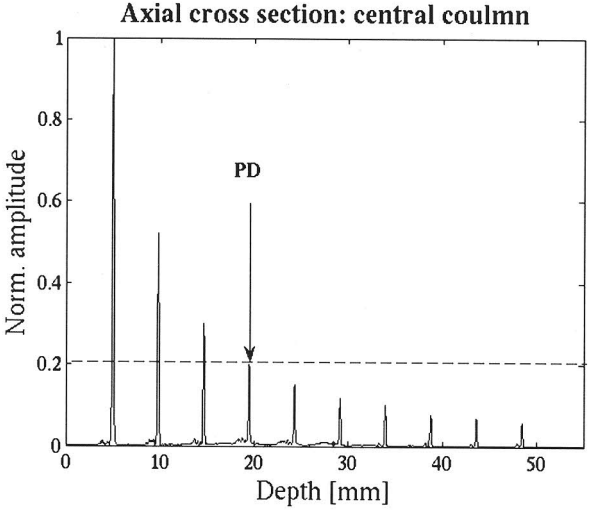

Fig. 3 Evaluation of the penetration depth: PD is the location of deepest reflector for which the normalized amplitude exceeds the chosen minimum threshold level in the axial cross section coinciding with the central phantom column

In the case when the lateral resolution is of main concern, the algorithm in the first step seeks for the transmit aperture size yielding the best lateral resolution, that is the minimum value of the LR parameter defined in Fig. 2b. This configuration is supplemented with the ones giving the lateral resolutions which fall within certain defined tolerance limit. In the examples considered in the next section the decrease limit of the lateral resolution is assumed to be 15% of its maximum value. From this set of transmit aperture configurations the one is selected which yields the maximum penetration depth.

In the case of the second approach the value of main importance is the penetration depth. So, in the first place the algorithm seeks for the transmit aperture yielding the maximum penetrations depth. This configuration is supplemented with the ones giving the penetration depth not less then certain defined minimum acceptable limit. In the example considered further this decrease is chosen to be 15% of the maximum value. From this set of transmit aperture configurations the one is selected, which yields the best lateral resolution. If more than one has been chosen (it is less likely to happen for larger number of image lines per pitch, which directly follows from the LR definition, see Fig. 2b) then the one with the largest aperture size or, alternatively, the one giving the best frame rate (minimum number of transmissions) is picked up.

4 Numerical Results and Discussion

In this section some numerical results illustrating the optimization algorithm performance are presented. The 128-element transducer with the pitch of 0.48 mm and the inter-element space of 0.15 mm excited by one sine cycle burst

Table 1 Aperture width for different visualization depth: approach 1

D, mm	5	10	15	20	25	30	35	40	45	50
N_t	1	1	2	2	3	3	3	4	4	4
δLR, %	45	52	22	16	5	12	11	–	–	–

Table 2 Aperture width for different visualization depth: approach 2

D, mm	5	10	15	20	25	30	35	40	45	50
N_t	1	2	2	3	3	3	4	4	4	4
δLR, %	45	32	22	–	5	12	–	–	–	–

pulse of the nominal frequency of 5 MHz with the sample rate of 50 MHz is considered. The thin wire phantom data are simulated by FIELD II program. As it was mentioned in the previous section the reflectors are located in the nodes of rectangular grid comprising ten equidistantly spaced rows and three columns. The central vertical line coincides with the transducer aperture center. The intervals between the columns and rows are 15 and 5 mm, respectively. The MSTA algorithm with $N_{sh} = N_t$ yielding the maximum frame rate increase as compared to the STA algorithm is considered.

In Table 1 the optimized values of the transmit aperture width N_t are shown for different visualization depths. The results correspond to the case of optimization approach selecting the configuration with maximum penetration depth from within the set of transmit apertures yielding the lateral resolution decrease less than 15% of its maximum value.

The configuration which yields the maximum penetration depth is the one with $N_t = 4$. For this case the decrease of the lateral resolution as compared to the optimized value of N_t at different depths is shown in the last row in Table 1. The best lateral resolution is achieved by the STA algorithm, but only for low visualization depths. On the other hand, the case of $N_t = 4$ enables visualization of the deepest parts of the phantom, but at the cost of lateral resolution deterioration at lower depths as compared to STA method. In Table 2 the optimization results corresponding to the second approach, selecting the configuration which yields the best lateral resolution for experiments with penetration depth not less than 15% of the maximum value are shown.

Comparison of the results in Tables 1 and 2 reveals a similarity of the optimal transmit aperture configurations obtained by two different approaches.

In Fig. 4 the lateral cross sections at the depths 10, 20, 30, and 40 mm, corresponding to different optimal transmit aperture configurations, are shown. For comparison the cases of $N_t = 1$–4 are illustrated. From Fig. 4 it is clear that for row 2 of the phantom (10 mm depth) the optimal lateral resolution is achieved by STA algorithm, whereas at the depths of 20 mm and deeper the larger transmit apertures are the best choice. And below the depth of 30 mm the best overall quality – the lateral resolution and penetration depth – is yielded by the transmit aperture with $N_t = 4$. This can be seen in Fig. 5 where the axial cross sections of the central column of the phantom are shown for different depths. Apparently, at the depths not exceeding 15–20 mm the smaller transmit apertures give better

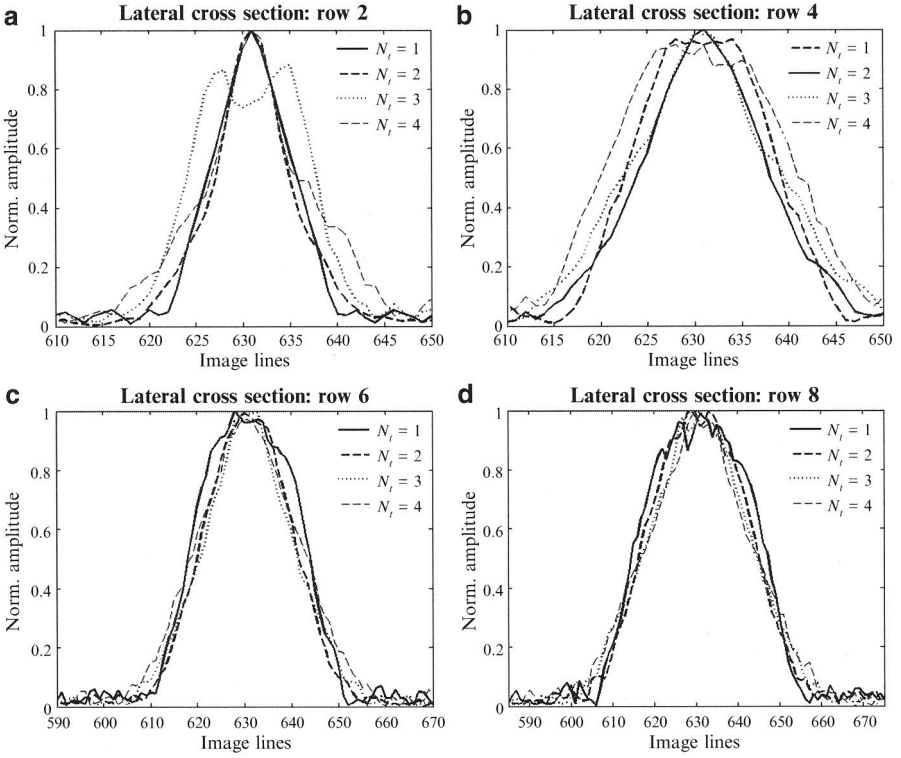

Fig. 4 Comparison of the lateral cross sections at different depths: (**a**) 10 mm (phantom row 2), (**b**) 20 mm (phantom row 4), (**c**) 30 mm (phantom row 6), (**d**) 40 mm (phantom row 8)

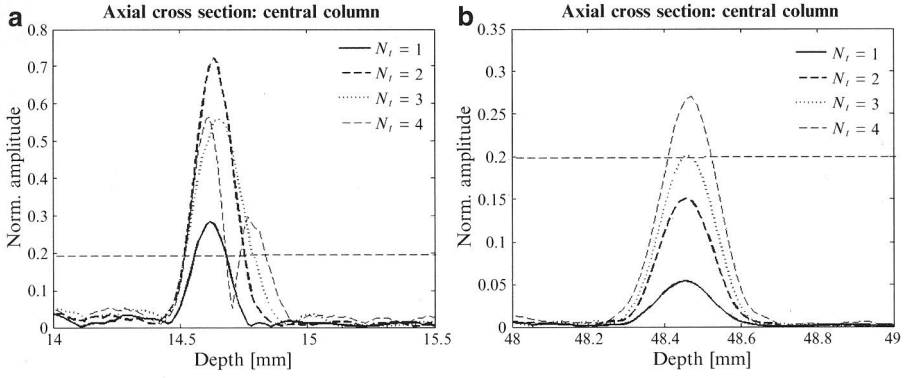

Fig. 5 Comparison of the axial cross sections of the phantom central column for different depths corresponding to: (**a**) row 3 and (**b**) row 10 of the phantom

lateral resolution. To visualize the deeper parts of the phantom the larger apertures should be chosen, which allows to increase the frame rate at the same time. Thus, if the main concern is the penetration depth together with the frame rate increase and some decrease in the lateral resolution is acceptable, than it is reasonable to use the MSTA algorithm with optimal number of elements $N_t = 4$ (in the considered example) to the whole range of visualization depths.

5 Conclusions

The work presents the investigation of the multi-element transmit aperture algorithm (MSTA) for ultrasound imaging. The main concern of the paper is the optimal choice of transmit aperture size providing the best compromise between the lateral resolution and penetration depth of the resulting 2D ultrasound image. For this purpose the corresponding optimization algorithm has been developed. Two different approaches have been implemented and compared which appeared to give similar results. The first one selects the configuration with the best penetration depth and the lateral resolution within some tolerance range, whereas the second one selects the transmit aperture yielding the best lateral resolution for penetration depth not less than some minimum acceptable value. A thin wire phantom and 128-element linear transducer array excited by a sine cycle burst of the nominal frequency of 5 MHz simulated in the FIELD II program were used in the numerical examples. For the test phantom the best image quality as concerns the lateral resolution at low depths of 10–20 mm is achieved by the small apertures with $N_t = 1, 2$. On the other hand, the deeper phantom regions are better visualized if the transmit aperture width $N_t = 4$ is selected. In the paper the MSTA algorithm with transmit aperture shift equal to its size was considered. However, the case with $N_{sh} < N_t$, which is characterized by somewhat better imaging quality but worse frame rate as compared to the $N_{sh} = N_t$, can be also treated by the approach. This, however, requires some modification of the optimization criteria and is a problem for future study.

Acknowledgements This work was supported by the Polish Ministry of Science and Higher Education (Grant NN518418436).

References

1. Holm, S., Yao, H.: Method and apparatus for synthetic transmit aperture imaging. US patent No 5.951.479, 14 Sept 1999
2. Daher, N.M., Yen, J.T.: 2-D array for 3-D ultrasound imaging using synthetic aperture techniques. IEEE Trans. Ultrason. Ferroelectr. Freq. Control **53**(5), 912–924 (2006)
3. Trots, I., Nowicki, A., Lewandowski, M.: Synthetic transmit aperture in ultrasound imaging. Arch. Acoust. **34**(4), 685–695 (2009)

4. Gammelmark, K.L., Jensen, J.A.: Multielement synthetic transmit aperture imaging using temporal encoding. IEEE Trans. Med. Imaging **22**(4), 552–563 (2003)
5. Trots, I., Nowicki, A., Lewandowski, M., Tasinkevych, Y.: Multi-element synthetic transmit aperture in medical ultrasound imaging. Arch. Acoust. **35**(4), 687–699 (2010)
6. Jensen, J.A.: Field: a program for simulating ultrasound systems. In Paper presented at the 10th Nordic-Baltic Conference on Biomedical Imaging Published in Medical & Biological Engineering & Computing. **34**(Suppl. 1, Part 1), 351–353 (1996)
7. Jensen, J.A., Svendsen, N.B.: Calculation of pressure fields from arbitrarily shaped, apodized, and excited ultrasound transducers. IEEE Trans. Ultrason. Ferroelectr. Freq. Control **39**, 262–267 (1992)